Characterization of the Angular Orientation Distribution of Discotic Molecules in Thin-Film Assemblies: Combinations of Polarized Transmission and Reflection−Absorption Infrared Spectroscopies

Niranjani Kumaran,‡ Carrie L. Donley,†,‡ Sergio B. Mendes,*,‡,§ and Neal R. Armstrong*,‡

Department of Chemistry, University of Arizona, Tucson, Arizona 85721, and Department of Physics & Astronomy, University of Louisville, Louisville, Kentucky 40292

We present a protocol to determine the angular orientation of surface-confined discotic molecules in ordered thin-film assemblies through a combination of polarized reflection absorption infrared spectroscopy (RAIRS) and polarized transmission infrared (IR) spectroscopy. We focus here on the determination of the orientation of side-chain-modified disk-like phthalocyanine molecules that self-organize to form parallel columnar aggregates in Langmuir−Blodgett (LB) films. This work complements and follows on work published previously (*Langmuir* **2005,** *21,* 360−368) where we used the visible absorbance dichroism in similar assemblies to determine the tilt angles of discotic molecules. The approach described here is applicable to all disk-like molecules that possess distinct in-plane or out-of-plane IR transitions. Molecular orientation is determined by comparison of absorbance intensities that are measured using (*i*) a RAIRS spectrum of the thin-film material on a gold surface, (*ii*) transmission spectra taken at two different polarizations of the thin-film material on an IR-transparent silicon substrate, and (*iii*) a transmission IR spectrum of an isotropic sample. We chose two distinct IR transitions of this molecule (a C−O−C "in-plane" stretch, ν_{C-O-C}, and a C−H out-of-plane bend, δ_{C-H}), which we initially assume are orthogonal to each other. The ν_{C-O-C} transition is modeled as an in-plane circular dipole, and the δ_{C-H} transition is modeled as a linear out-of-plane dipole. Formalisms are described that allow the determination of two independent values for order parameters within the thin film using the dichroism in these transitions in all three IR spectra, assuming that the microstructure of these thin films is the same on both the gold and silicon substrates. The spectra from the δ_{C-H} transition appear to best describe the orientation of these molecules within the molecular assembly, these IR results agreeing best with earlier visible absorbance and X-ray diffraction studies. The preferential alignment of the δ_{C-H} transition is parallel to the substrate, arising from *Pc* molecules that are nearly upright, edge-on to the substrate plane. The approach described here provides a means of complete description of the tilt angles of the monomer building blocks in any discotic assembly in thin-film formats, where distinct in-plane and out-of-plane optical transitions are available.

Introduction

Discotic molecular assemblies continue to show great potential as molecular electronic materials because of their tendency to form coherent linear aggregates, with strong overlap of adjacent molecular cores, providing for high charge mobilities along the rod-like aggregate axis.[1−19] In applications where these linear aggregates are formed with the rod axis parallel to the substrate plane, such as would be required for organic field effect transistors (OFET),[9,13,15,16,20,21] it is apparent that the microstructure in these films, as evidenced by the tilt angles of the discotic building blocks in these aggregates, will play a role in determining the charge mobilities.[5,6,17,22] Because the arene−arene interactions, which control hopping of charges between discotic centers, are strongly affected by even small changes in tilt angles and the atomic positions of atoms in adjacent molecules,[5,17,22,23] it is essential to have ways of determining

these tilt angles, and their angular distributions, on substrates that model those used in OFETs and related technologies.

We have shown previously that the dichroism in the visible absorbance spectra of discotic assemblies, especially those based on octa-alkoxy or octa-thioether phthalocyanines,[12−14] can be used to determine the order parameters related to the tilt angles of the chromophores, provided that polarized light is used on waveguide substrates that allow interrogation of absorbance dichroism both parallel to and perpendicular to the long axis of the rod-like aggregate thin films.[24] The majority of those studies were focused on 2,3,9,10,16,17,23,24-octakis((2-benzyloxy)-ethoxy)phthalocyaninato copper (II) (**Pc 1**, Figure 1) which forms coherent linear aggregates, transferred as Langmuir−Blodgett films to a variety of substrates, without loss in film coherence.[25]

Infrared absorbance dichroism can also be used to characterize these thin films, but in this case distinct vibrational bands are sought, preferably those whose transition dipoles are either in the molecular plane (e.g., the C−O−C stretch, ν_{C-O-C}) or perpendicular to the molecular plane (e.g., the C−H out-of-plane bend, δ_{C-H}).[13,15,25,26] Our earlier studies showed the necessity to combine both reflection−absorption measurements

* Corresponding authors. E-mail: sbmend01@louisville.edu; nra@u.arizona.edu.
† Current Address: Institute for Advanced Materials, NanoScience & Technology, University of North Carolina, Chapel Hill, NC 27599.
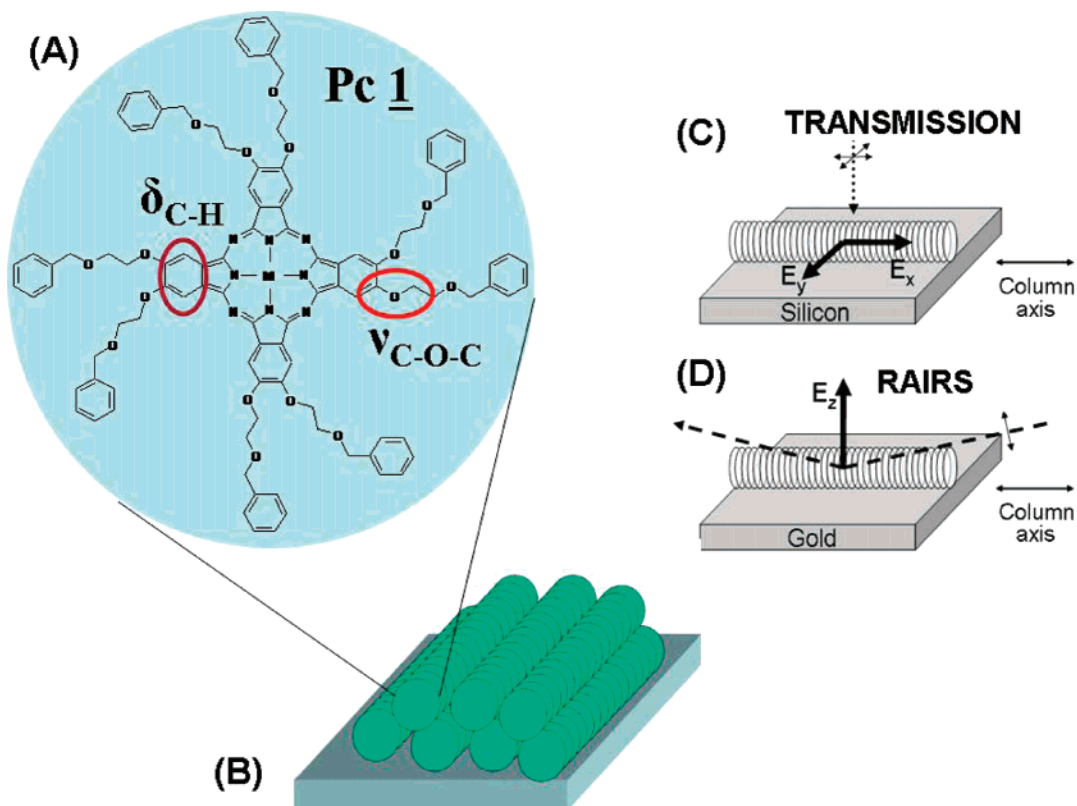‡ University of Arizona.
§ University of Louisville.

Figure 1. (A) Schematic view of **Pc 1**, showing the in-plane ν_{C-O-C} and out-of-plane δ_{C-H} transitions; (B) schematic view of the rod-like aggregates formed from this type of discotic material (see AFM images in refs 13 and 24), showing the distinct rod axis, parallel to the compression direction on the LB trough; (C) the laboratory coordinates and the electric field vectors produced by transmission; and (D) RAIRS experiments in relation to the Pc column aggregate axis. In both experiments, the substrate plane is defined as the $x-y$ plane with the column axis defined as the x direction. Infrared transitions with components along the x and y axes are probed in the transmission experiment, whereas transitions with components along the z axis are probed in the RAIRS experiment.

(RAIRS) on gold substrates and transmission measurements on IR-transparent silicon to determine Pc orientation. As will be shown here, these earlier attempts to estimate the tilt angle of the individual molecules made simplifying assumptions, based on previous studies of linear rather than discotic molecular systems,[27−29] which may be problematic for a full description of the structure of a discotic molecular assembly thin film.

In this paper, we propose a simple method to determine the angular orientation of any disk-like molecule using infrared spectroscopy in a combination of transmission and reflection−absorption modes. We chose thin films of **Pc 1** to serve as the model system in this study because its microscopic and macroscopic film structure has been well characterized by a combination of spectroscopies, X-ray diffraction, and atomic force microscopy,[12−14,24,25,30] although in theory any discotic molecule with distinct in-plane and out-of-plane IR transitions could be the target for such an investigation (e.g., triphenylenes, hexabenzocoronene, etc.). For Pc molecules with D_{4h} symmetry, rotation about the molecular axis α (Figure 2) gives the same spectroscopic results and thus forms an optically circular absorber. Information on angular orientation of the discotic molecule through order parameters associated with the tilt angle, θ, (angle between molecular axis and the sample normal) and the twist angle, Φ, (rotation about the sample surface normal) are the focus of these studies.

Although several previous reports have described infrared spectroscopic methods, using polarized light sources, to determine the orientation of molecules on surfaces, very few have addressed discotic molecules.[26,28,31] Of the studies involving discotic molecules, assumptions were made to simplify the system, leaving only a single-order parameter to be determined.
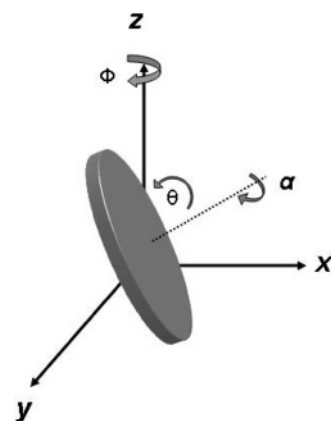

Figure 2. Schematic illustration of the possible angular rotations in a disk-like molecule. The molecules exhibit a tilt away from the substrate plane (θ) (or the tilt angle between the sample normal and the normal to the molecular plane), a twist about the surface normal (Φ), and a rotation about the normal of the molecular plane (α).

Debe considered the use of reflection absorption IR spectroscopy (RAIRS) to study the ordering of vacuum-deposited hydrogen Pc (H_2Pc), but this treatment only applies to molecules with D_{2h} symmetry[28] and cannot be used for molecules with D_{4h} symmetry, the symmetry of most metal-substituted phthalocyanines. Also, because data was only obtained in the RAIRS geometry, they could only assign a tilt angle of the molecules away from the surface normal. Sauer et al. used polarized transmission IR spectroscopy to determine the orientation of polymeric silicon phthalocyanines (linked by central O−Si−O−Si bonds, PcPS) on IR-transparent substrates.[26] The O−Si−

O−Si backbone of PcPS forces the Pcs in the polymer chain into a perpendicular orientation with respect to the surface; and because they are also perpendicular (on average) to the PcPS column axis, only the direction of the column was left to be determined.[26] For the Pc molecules in the horizontally trans-ferred Langmuir−Blodgett (LB) films studied here, there is no a priori justification for the assumption above. To fully define the order parameters of a surface-confined discotic molecule, spectroscopic measurements of absorbance dichroism must be made in three orthogonal directions with respect to the laboratory frame of reference.

In this paper, we present the expanded version of our previous IR studies of discotic molecular systems. The protocol combines a polarized transmission experiment, which is performed at a normal angle of incidence on an IR-transparent substrate (silicon), and a RAIRS experiment, which is made at a high angle of incidence on a highly reflective (gold) substrate. We assumed that the molecular assembly adopts the same macro-scopic and microscopic orientation on both substrates because similar surface modifications are used for each substrate, and horizontally transferred LB films of **Pc 1** are stiff and easily transferred to a number of substrates, and quite coherent, with similar structures, on both modified gold and modified single-crystal silicon.[13,14] By employing both polarized transmission IR and RAIRS experiments, the electric field component of the incident radiation can be produced along each of three axes to probe vibrational transitions in directions E_z in the RAIRS experiment and E_x and E_y in the transmission experiment. In addition, spectra of an isotropic sample, powders of **Pc 1** dispersed in KBr pellets, were used to determine the relative strengths of the transition dipoles. **Pc 1** is initially modeled as having a circular, in-plane vibrational dipole and an out-of plane vibrational dipole that is perpendicular to the circular dipole. By addressing the two distinct transitions, ν_{C-O-C} and δ_{C-H}, measured simultaneously, two independent probes of molecular orientation result, which subsequently allow us to check the consistency of the model proposed. In order to validate our theory, we apply these calculations to thin films of **Pc 1** that were prepared in two different methods, LB films and spin cast films, both of which are expected to have slight variation in molecular ordering.

Theory

Schematic drawings showing the lab coordinate axes and the geometry for the reflection and transmission experiments are shown in Figures 1 and 2. Films of the **Pc 1** molecules were deposited so that the Pc rod axis was parallel to the LB trough compression barrier axis,[13,25] which was defined as the x axis. The stiff nature of these films, horizontally transferred to the substrate, makes it possible to assume equivalent orientations on both silicon and gold substrates. The $x-y$ plane defines the substrate plane, with the z axis normal to the substrate. In the transmission experiment, the incident IR beam (Figure 1d) was perpendicular to the substrate (normal incidence) and could be polarized along either the x or y axis. The incident IR beam in the reflection experiment (Figure 1d) is incident at 80° from the sample normal. The incident beam in the RAIRS experiment was p-polarized.

We first consider a system with in-plane ("in") and out-of-plane ("out") transition bands. The square of the strength of each dipole is equal to the sum of the squares of the strength of this dipole projected along each of the coordinate axes

$$\mu_{in}^2 = \langle\mu_{x,in}^2\rangle + \langle\mu_{y,in}^2\rangle + \langle\mu_{z,in}^2\rangle \tag{1}$$

$$\mu_{out}^2 = \langle\mu_{x,out}^2\rangle + \langle\mu_{y,out}^2\rangle + \langle\mu_{z,out}^2\rangle \tag{2}$$

where $\mu_{i,in}^2$ and $\mu_{i,out}^2$ are the in- and out-of-plane dipoles along the i axis and the brackets indicate the ensemble average over the sample region probed by the optical beam. We define the ratio

$$f \equiv \frac{\mu_{in}^2}{\mu_{out}^2} \tag{3}$$

where f is the absorbance ratio of the two transition bands determined from transmission measurements made for an isotropic sample (powders of **Pc 1** in a KBr pellet).

The transmission measurements for thin films of the Pc on IR-transparent silicon allow the absorbance of both transitions along the x and y axes to be measured. The absorbance from the in-plane transition band along each of these axes can be expressed as follows:

$$A_{x,in} = \langle\mu_{x,in}^2\rangle E_{tr}^2 \tag{4}$$

$$A_{y,in} = \langle\mu_{y,in}^2\rangle E_{tr}^2 \tag{5}$$

E_{tr}^2 is the strength of the electric field in the transmission experiment. Similarly, the absorbance due to the out-of-plane transition band can be expressed as

$$A_{x,out} = \langle\mu_{x,out}^2\rangle E_{tr}^2 \tag{6}$$

$$A_{y,out} = \langle\mu_{y,out}^2\rangle E_{tr}^2 \tag{7}$$

In the RAIRS measurement, the electric field in the thin-film sample close to the metal surface is essentially along the z axis and the absorbance of the in-plane and out-of-plane transition bands are described by the following

$$A_{z,in} = \langle\mu_{z,in}^2\rangle E_z^2 \tag{8}$$

$$A_{z,out} = \langle\mu_{z,out}^2\rangle E_z^2 \tag{9}$$

Then by combining eqs 4 and 5

$$A_{x,in} + A_{y,in} = \{\langle\mu_{x,in}^2\rangle + \langle\mu_{y,in}^2\rangle\}E_{tr}^2 \tag{10}$$

and combining eqs 6 and 7

$$A_{x,out} + A_{y,out} = \{\langle\mu_{x,out}^2\rangle + \langle\mu_{y,out}^2\rangle\}E_{tr}^2 \tag{11}$$

We next define the term g

$$g \equiv \frac{A_{x,in} + A_{y,in}}{A_{x,out} + A_{y,out}} \tag{12}$$

and then consider eqs 1, 2, 10, and 11 into 12 to arrive at the following expression:

$$g = \frac{\langle\mu_{x,in}^2\rangle + \langle\mu_{y,in}^2\rangle}{\langle\mu_{x,out}^2\rangle + \langle\mu_{y,out}^2\rangle} = \frac{\mu_{in}^2 - \langle\mu_{z,in}^2\rangle}{\mu_{out}^2 - \langle\mu_{z,out}^2\rangle} \tag{13}$$

By substituting eqs 3, 8, and 9 into 13

$$g = \frac{f\mu_{out}^2 - \frac{A_{z,in}}{A_{z,out}}\langle\mu_{z,out}^2\rangle}{\mu_{out}^2 - \langle\mu_{z,out}^2\rangle} = \frac{f - \frac{A_{z,in}}{A_{z,out}}\frac{\langle\mu_{z,out}^2\rangle}{\mu_{out}^2}}{1 - \frac{\langle\mu_{z,out}^2\rangle}{\mu_{out}^2}} \qquad (14)$$

We then define a parameter h

$$h \equiv \frac{A_{z,in}}{A_{z,out}} = \frac{\langle\mu_{z,in}^2\rangle}{\langle\mu_{z,out}^2\rangle} \qquad (15)$$

which when inserted into eq 14 gives us

$$\frac{\langle\mu_{z,out}^2\rangle}{\mu_{out}^2} = \frac{f - g}{h - g} \qquad (16)$$

By using eqs 3, 15, and 16, we obtain

$$\frac{\langle\mu_{z,in}^2\rangle}{\mu_{in}^2} = \left(\frac{f - g}{h - g}\right)\frac{h}{f} \qquad (17)$$

Now, when combining eqs 1 and 17 we get

$$\frac{\langle\mu_{x,in}^2\rangle}{\mu_{in}^2} + \frac{\langle\mu_{y,in}^2\rangle}{\mu_{in}^2} = 1 - \frac{\langle\mu_{z,in}^2\rangle}{\mu_{in}^2} = \left(\frac{h - f}{h - g}\right)\frac{g}{f} \qquad (18)$$

By defining an absorbance ratio for the in-plane transitions

$$R_{in} \equiv \frac{A_{y,in}}{A_{x,in}} = \frac{\langle\mu_{y,in}^2\rangle}{\langle\mu_{x,in}^2\rangle} \qquad (19)$$

then

$$\frac{\langle\mu_{x,in}^2\rangle}{\mu_{in}^2} + \frac{R_{in}\langle\mu_{x,in}^2\rangle}{\mu_{in}^2} = \left(\frac{h - f}{h - g}\right)\left(\frac{g}{f}\right) \qquad (20)$$

which leads to

$$\frac{\langle\mu_{x,in}^2\rangle}{\mu_{in}^2} = \left(\frac{h - f}{h - g}\right)\left(\frac{g}{f}\right)\left(\frac{1}{1 + R_{in}}\right) \qquad (21)$$

and

$$\frac{\langle\mu_{y,in}^2\rangle}{\mu_{in}^2} = \left(\frac{h - f}{h - g}\right)\left(\frac{g}{f}\right)\left(\frac{R_{in}}{1 + R_{in}}\right) \qquad (22)$$

Similarly for the out-of-plane transition by defining an absorbance ratio

$$R_{out} \equiv \frac{A_{y,out}}{A_{x,out}} = \frac{\langle\mu_{y,out}^2\rangle}{\langle\mu_{x,out}^2\rangle} \qquad (23)$$

and using eqs 2 and 16 we obtain

$$\frac{\langle\mu_{x,out}^2\rangle}{\mu_{out}^2} = \left(\frac{h - f}{h - g}\right)\left(\frac{1}{1 + R_{out}}\right) \qquad (24)$$

$$\frac{\langle\mu_{y,out}^2\rangle}{\mu_{out}^2} = \left(\frac{h - f}{h - g}\right)\left(\frac{R_{out}}{1 + R_{out}}\right) \qquad (25)$$

Equations 16, 17, 21, 22, 24, and 25 relate the strength of a dipole along one particular axis (the ratio between the average of the squared dipole projections along a coordinate axis and the squared total dipole strength) to experimentally measured parameters. Once a model relating the geometry of these dipoles to each other and to the molecular structure is defined, these expressions lead to the desired orientation information.

In proposing a model for the phthalocyanine molecule, we have made three assumptions: (*i*) a circular dipole, μ_{in}, arises from the eight $v_{(Pc-O-C, ip)}$ stretching vibrations, distributed about the Pc core, (*ii*) there is a linear dipole, μ_{out} due to the vibration of aromatic hydrogens ($\delta_{(ring C-H, op)}$) attached directly to the Pc core, and (*iii*) these dipoles are perpendicular to each other. Then we can write

$$\begin{pmatrix}\mu_x\\\mu_y\\\mu_z\end{pmatrix} = \begin{pmatrix}\cos\phi & -\sin\phi & 0\\\sin\phi & \cos\phi & 0\\0 & 0 & 1\end{pmatrix}\begin{pmatrix}1 & 0 & 0\\0 & \cos\theta & -\sin\theta\\0 & \sin\theta & \cos\theta\end{pmatrix}$$
$$\begin{pmatrix}\cos\alpha & -\sin\alpha & 0\\\sin\alpha & \cos\alpha & 0\\0 & 0 & 1\end{pmatrix}\begin{pmatrix}\mu_{in}/\sqrt{2}\\\mu_{in}/\sqrt{2}\\\mu_{out}\end{pmatrix} \qquad (26)$$

from which the following equations result when the expressions are integrated over 0 to 2π in α (circular dipole).

$$\frac{\langle\mu_{x,in}^2\rangle}{\mu_{in}^2} = \frac{1}{2}\{\langle\cos^2\phi\rangle + \langle\sin^2\phi\cos^2\theta\rangle\} \qquad (27)$$

$$\frac{\langle\mu_{y,in}^2\rangle}{\mu_{in}^2} = \frac{1}{2}\{\langle\sin^2\phi\rangle + \langle\cos^2\phi\cos^2\theta\rangle\} \qquad (28)$$

$$\frac{\langle\mu_{z,in}^2\rangle}{\mu_{in}^2} = \frac{1}{2}\langle\sin^2\theta\rangle \qquad (29)$$

$$\frac{\langle\mu_{x,out}^2\rangle}{\mu_{out}^2} = \langle\sin^2\phi\sin^2\theta\rangle \qquad (30)$$

$$\frac{\langle\mu_{y,out}^2\rangle}{\mu_{out}^2} = \langle\cos^2\phi\sin^2\theta\rangle \qquad (31)$$

$$\frac{\langle\mu_{z,out}^2\rangle}{\mu_{out}^2} = \langle\cos^2\theta\rangle \qquad (32)$$

Thus for the model employed here, the in-plane transition dipole components ($\langle\mu_{i,in}^2\rangle/\mu_{in}^2$) can take on values between 0 and 0.5 while the out-of-plane components ($\langle\mu_{i,out}^2\rangle/\mu_{out}^2$) can range from 0 to 1.

Equation 27 can be rearranged to compare its experimental result with the one provided by eq 30:

$$\langle\sin^2\phi\sin^2\theta\rangle = \frac{\langle\mu_{x,out}^2\rangle}{\mu_{out}^2} = 1 - \frac{2\langle\mu_{x,in}^2\rangle}{\mu_{in}^2} \qquad (33)$$

Similarly, eqs 28 and 31 give us

Angular Orientation Distribution

J. Phys. Chem. C, Vol. 112, No. 13, 2008 **4975**

$$\langle \cos^2 \phi \sin^2 \theta \rangle = \frac{\langle \mu_{y,\text{out}}^2 \rangle}{\mu_{\text{out}}^2} = 1 - \frac{2\langle \mu_{y,\text{in}}^2 \rangle}{\mu_{\text{in}}^2} \qquad (34)$$

and eqs 29 and 32

$$\langle \cos^2 \theta \rangle = \frac{\langle \mu_{z,\text{out}}^2 \rangle}{\mu_{\text{out}}^2} = 1 - \frac{2\langle \mu_{z,\text{in}}^2 \rangle}{\mu_{\text{in}}^2} \qquad (35)$$

In eqs 33−35, the molecular orientation parameters (left-hand side) can be calculated either by the out-of-plane transition or by the in-plane (circular) transition. Therefore, if the assumptions above are correct then both results should agree within experimental uncertainties.

Experimental Section

2,3,9,10,16,17,23,24-Octakis((2-benzyloxy)ethoxy)phthalo-cyaninato copper (II) (**Pc 1**), was synthesized as reported previously.[32] Solutions of this molecule were prepared in HPLC-grade CHCl$_3$ stabilized with ethanol (Aldrich).

1,1,1,3,3,3-Hexamethyldisilazane and 1,3-diphenyl-1,1,3,3-tetramethyldisilazane were purchased from Aldrich and used without further purification, and benzyloxyethane thiol was synthesized in our lab as reported previously.[25] Silicon (100) surfaces were cleaned by immersing in Klean AR (93% sulfuric acid and 0.4% chromium trioxide, Mallinckrodt) for a few minutes and then rinsing with copious amounts of water. These surfaces were then hydrophobized by sonicating the clean surface in a disilane mixture (50:50) of 5% 1,1,1,3,3,3-hexamethyldisilazane and 5% 1,3-diphenyl-1,1,3,3-tetrameth-yldisilazane CHCl$_3$ for 30 min with heating.[15,25,30] Au surfaces were cleaned by immersing the surface into a piranha solution (4:1 H$_2$SO$_4$/H$_2$O$_2$) and then modified by soaking clean Au in a 1 mM solution of benzyloxyethane thiol in ethanol for at least 24 h. *Caution: piranha reacts violently with many organic compounds and should be handled with care.*

A Riegler & Kerstein RK3 Langmuir−Blodgett (LB) trough was used to form LB films by applying a solution of the molecules to the air−water interface, allowing the CHCl$_3$ solvent to evaporate, and then compressing the barriers.[12−15,25] Following film compression, the molecular columns are oriented parallel to the compression barriers, allowing for control of the orientation of the columns with respect to the substrate during film transfer.[13−15,25] A Wilhemy balance was used to measure the pressure at a position centered between the barriers. After film compression, the film was lowered onto a metal baffle placed underneath the surface of the water by removing some of the water in the sub phase. Contact of the rigid film to this baffle served to segment the film into 15 equal-sized pieces and allowed for horizontal (Schaefer) film transfer from one section without disturbing adjacent sections of the film. Film transfer by the horizontal transfer technique has been shown to give more ordered Pc films than the vertical transfer technique and has been used in all of these studies.[13−15,25] Four layers were deposited, one bilayer at a time, onto modified gold or silicon substrates, removing any residual water from the sample with a stream of N$_2$ between each transfer step. Finished films were annealed at 120 °C for at least 4 h to remove any residual water and to impart more order in the film by raising their temperature above their liquid crystal transition temperature (ca. 70 °C). KBr pellets were prepared by grinding 1 mg of **Pc 1** with 1 g of solid potassium bromide. Spin-coated samples were prepared on modified gold and hydrophobized silicon substrates by spinning 1 mM solution at 3000 rpm.

FT-IR transmission and reflection absorption infrared spectra (RAIRS) were obtained with a dry-air purged Nicolet 550 spectrometer with a globar IR source (EverGlo) and a liquid-nitrogen-cooled MCT detector. A gold wire grid polarizer (Cambridge Physical Sciences) was used in transmission experiments, where spectra were taken with the incident beam normal to the substrate and the polarizer oriented parallel or perpendicular to the Pc column axis. RAIRS spectra were obtained with a FT-80 fixed 80° grazing angle accessory (Spectra-Tech) with a p polarizer (ZnSe, manual polarizer).

Results and Discussion

Figure 3 shows both the transmission and RAIRS spectra for **Pc 1**. Figure 3a shows the transmission spectrum for the isotropic powder of **Pc 1** in a KBr pellet. Figure 3c and d shows the transmission spectra for a thin film of **Pc 1** on surface-modified IR-transparent silicon, while Figure 3b shows the RAIRS spectrum for the same thickness **Pc 1** films on modified Au. Although there are clear changes in the relative intensity of several peaks, we have focused mainly on two peaks that are assumed to have transition dipoles perpendicular to each other, both of which are marked with an "*" in Figure 3. We use the absorbance $v_{(\text{Pc}-\text{O}-\text{C, ip})}$ at 1284 cm^{-1} as the in-plane transition and $\delta_{(\text{ring, C}-\text{H, op})}$ at 745 cm^{-1} as the out-of-plane transition. The narrow peak at 745 cm^{-1} is overlapped with another transition whose contribution is removed by subtraction, followed by baseline fitting to isolate the out-of-plane transition.

As expected for highly ordered Pc rods made up of Pc disks with a nearly upright orientation (with respect to the substrate plane), the transmission spectra show a strong and complementary dichroism in both the $v_{\text{Pc}-\text{O}-\text{C}}$ and $\delta_{\text{C}-\text{H}}$ bands, while the RAIRS spectra, using a polarized excitation source, show very little intensity in the background corrected $\delta_{\text{C}-\text{H}}$ band, versus the isotropic sample, and a high $v_{\text{Pc}-\text{O}-\text{C}}$ intensity. As has been noted previously, this result confirms the small extent of projection of the $\delta_{\text{C}-\text{H}}$ transition dipole onto the z axis.

These qualitative observations are confirmed quantitatively by calculating the strength of transition dipole components along each of the coordinate axes (eqs 16, 17, 21, 22, 24, and 25). These ratios are summarized in Table 1 for both LB films of **Pc 1** and spin-coated samples. Let us consider first the results for the LB films. The out-of plane $\delta_{\text{C}-\text{H}}$ dipole of the molecular mesophase is strongly aligned with the x axis ($\langle \mu_{x,\text{out}}^2 \rangle / \mu_{\text{out}}^2 = 0.74$) with a small component along the other in-plane direction ($\langle \mu_{y,\text{out}}^2 \rangle / \mu_{\text{out}}^2 = 0.23$) and a negligible component along the z axis ($\langle \mu_{z,\text{out}}^2 \rangle / \mu_{\text{out}}^2 = 0.02$). These values signify that the out-of-plane dipole is preferentially distributed along the x axis and the molecular plane is standing nearly perpendicular to the substrate plane. The in-plane transition $v_{\text{Pc}-\text{O}-\text{C}}$ dipole strength is very weak along the x direction ($\langle \mu_{x,\text{in}}^2 \rangle / \mu_{\text{in}}^2 = 0.13$), and is mainly confined and evenly distributed in the y−z plane ($\langle \mu_{y,\text{in}}^2 \rangle / \mu_{\text{in}}^2 = 0.46$ and $\langle \mu_{z,\text{in}}^2 \rangle / \mu_{\text{in}}^2 = 0.41$), which again is quite consistent with an upright disk aligned in the y−z plane. The agreement of the results above are quantified and tested in Table 2 where order parameters are calculated using both the out-of- and in-plane transitions; although not perfect, their satisfactory agreement reflects the consistency in our initial assumptions.

The results of the experiments described here can be compared with a similar experiment done with a single bilayer **Pc 1** film using Q-band absorbance dichroism in an ATR geometry.[24] These experiments resulted in values of 0.12 (±0.04), 0.30 (±0.08), and 0.6 (±0.1) for the dipole strengths in the x, y, and z directions, respectively. The in-plane x component is almost the same for both the visible and infrared
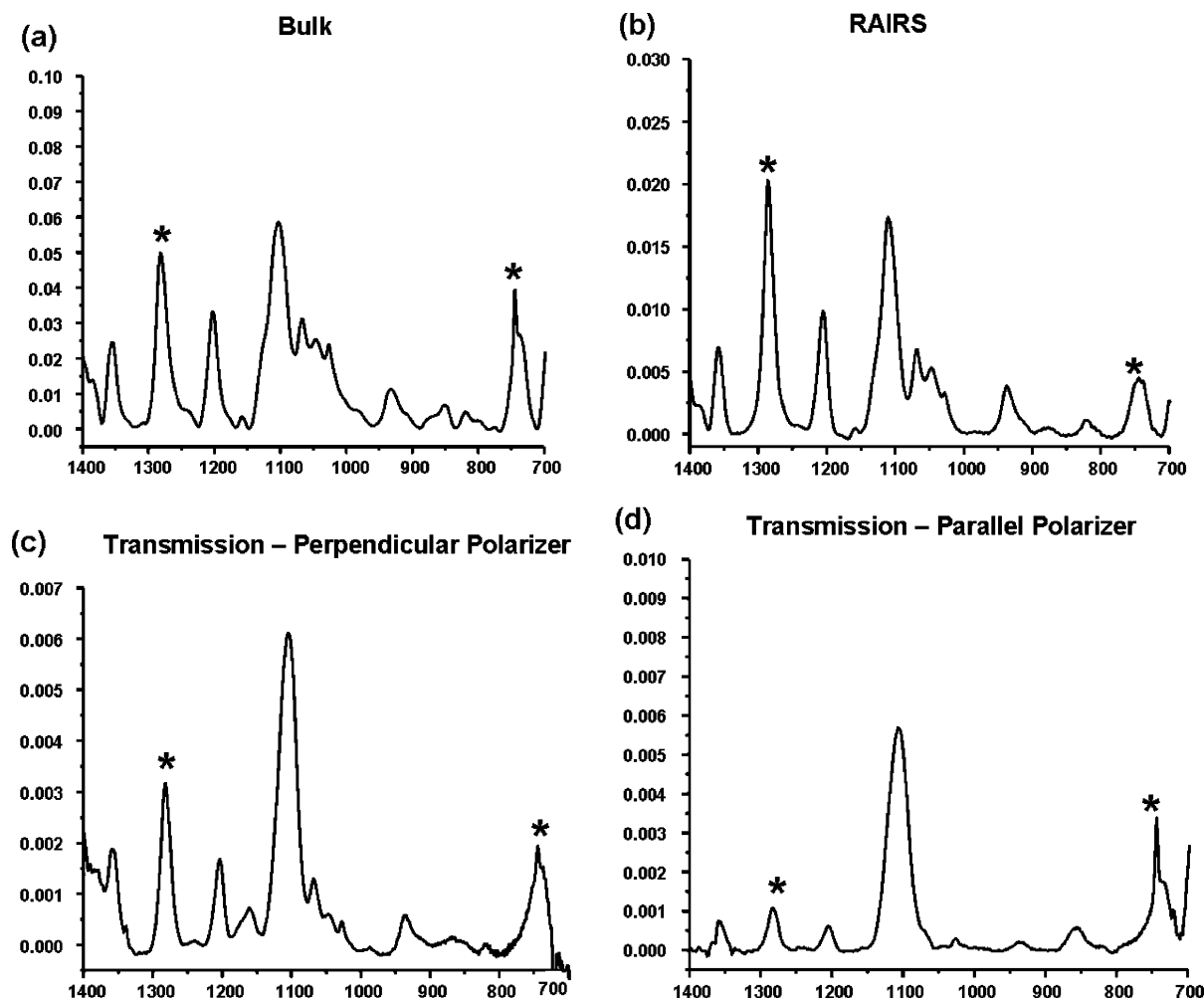
Figure 3. IR spectra of films of **Pc 1**. The asterisks in the spectra indicate the in-plane vibration at 1284 cm^{-1} and the out-of-plane vibration at 745 cm^{-1}. The four spectra show clear changes in relative intensity in the in-plane and out-of-plane peaks. (a) Transmission spectrum of Pc molecules dispersed in KBr pellet. (b) RAIRS spectrum of four bilayers of Pc on gold. (c and d) Transmission spectrum of four bilayers of Pc with a polarizer. (c) Polarizer oriented perpendicular and (d) polarizer oriented parallel to the column axis. In all of the spectra, absorbance is plotted against wave number (cm^{-1}).

TABLE 1: Relative Transition Dipole Strengths

sample	$\langle \mu_{x,out}^2 \rangle / \mu_{out}^2$	$\langle \mu_{y,out}^2 \rangle / \mu_{out}^2$	$\langle \mu_{z,out}^2 \rangle / \mu_{out}^2$	$\langle \mu_{x,in}^2 \rangle / \mu_{in}^2$	$\langle \mu_{y,in}^2 \rangle / \mu_{in}^2$	$\langle \mu_{z,in}^2 \rangle / \mu_{in}^2$
LB film	0.74 ± 0.009	0.23 ± 0.008	0.02 ± 0.006	0.13 ± 0.02	0.46 ± 0.06	0.41 ± 0.07
spin-coated film	0.46 ± 0.01	0.49 ± 0.01	0.05 ± 0.02	0.31 ± 0.04	0.29 ± 0.04	0.40 ± 0.07

TABLE 2: Comparison of Order-Parameters Measured from In- and Out-of-Plane Transition Dipoles

sample	eq 33 $\langle \sin^2\phi \sin^2\theta \rangle$		eq 34 $\langle \cos^2\phi \sin^2\theta \rangle$		eq 35 $\langle \cos^2\theta \rangle$	
	$\langle \mu_{x,out}^2 \rangle / \mu_{out}^2$	$1 - 2\langle \mu_{x,in}^2 \rangle / \mu_{in}^2$	$\langle \mu_{y,out}^2 \rangle / \mu_{out}^2$	$1 - 2\langle \mu_{y,in}^2 \rangle / \mu_{in}^2$	$\langle \mu_{z,out}^2 \rangle / \mu_{out}^2$	$1 - 2\langle \mu_{z,in}^2 \rangle / \mu_{in}^2$
LB film	0.74 ± 0.009	0.74 ± 0.008	0.23 ± 0.008	0.08 ± 0.005	0.02 ± 0.004	0.18 ± 0.002
spin-coated film	0.46 ± 0.01	0.38 ± 0.02	0.49 ± 0.01	0.42 ± 0.02	0.05 ± 0.02	0.2 ± 0.05

experiments, but differences between the *y* and *z* components observed in the visible spectra are not present in the infrared data. It should be pointed out that the visible ATR analysis described previously requires a precise characterization of the film birefringence;[24] that requirement is not needed in the RAIRS infrared data because only one Cartesian component (the *z* component) appears in the analysis. Such a distinction may turn the infrared approach described here less susceptible to additional experimental errors.

In order to further validate our methodology, we applied our theoretical approach and assumptions to a spin-coated sample. Unlike LB films, spin coating is expected to result in less-ordered molecular columnar aggregates in the sample plane

(*x* and *y* components), and we expect to get similar values of dipole strengths along those directions. Our assumption is confirmed successfully in our results (Table 1) for both in-plane and out-of-plane dipole strengths. The orientation distribution of the out-of-plane dipole in the spin-coated sample along the *z* direction (0.05) is similar to that which was observed in the LB film (0.02) but it has almost an equal amount of projections in both *x* and *y* directions. This indicates, that, although the molecules are standing upright in the spin-cast film, they are not well-ordered in the *x*−*y* plane. The in-plane transition of the spin-coated film, besides showing the expected in-plane symmetry, has strength along the *z* component (0.40), in excellent agreement with the LB films (0.41).

Angular Orientation Distribution

J. Phys. Chem. C, Vol. 112, No. 13, 2008 **4977**

If our assumption that the transition dipoles for the v_{Pc-O-C} and δ_{C-H} vibrations are perpendicular to each other is correct, then there should be a clear relationship between the dipole components. These relationships were evaluated in quantitative terms by comparing the results in eqs 33–35 calculated with the in- and out-of-plane transitions. The calculated results tabulated in Table 2 show a satisfactory agreement with these expressions and therefore support our initial assumption that the two transition dipoles are almost perpendicular to each other. In addition, as stated in the Theory section, if the in-plane transition is a circular dipole, then the in-plane transition components ($\langle \mu_{i,in}^2 \rangle / \mu_{in}^2$) can take on values between 0 and 0.5 whereas if the out-of-plane transition is a linear dipole, then its components ($\langle \mu_{i,out}^2 \rangle / \mu_{out}^2$) can range from 0 to 1. These conditions are well satisfied in our results and again show the consistency of the other two assumptions.

Conclusions

We have developed a technique combining reflection and transmission infrared spectroscopies to determine the relative dipole components along each of the laboratory axes. The relative strength of this dipole along each the laboratory axes showed that the orientation of the **Pc 1** molecules is upright in the LB film. Given the assessment of the assumptions made in this approach and comparison of the results with our previous work (*Langmuir* **2005**, *21*, 360–368), we suggest that this method, which probes specific vibrational transitions at the molecular level, may be more reliable than approaches that focus on the absorbance spectra of extended aggregates or X-ray diffraction or X-ray scattering studies that rely upon modeling of the thin-film microstructure. These rigid films of **Pc 1** are an unusually convenient test material with which to evaluate each of these approaches to the determination of molecular orientation. Our results here illustrate, however, that this approach should be applicable to study any ultrathin film of discotic molecules, where the individual mesogen possesses two distinct and perpendicular transition dipoles.

References and Notes

(1) Deibel, C.; Janssen, D.; Heremans, P.; De Cupere, V.; Geerts, Y.; Benkhedir, M. L.; Adriaenssens, G. J. *Org. Electron.* **2006**, *7*, 495.

(2) Tant, J.; Geerts, Y. H.; Lehmann, M.; De Cupere, V.; Zucchi, G.; Laursen, B. W.; Bjornholm, T.; Lemaur, V.; Marcq, V.; Burquel, A.; Hennebicq, E.; Gardebien, F.; Viville, P.; Beljonne, D.; Lazzaroni, R.; Cornil, J. *J. Phys. Chem. B* **2005**, *109*, 20315.

(3) Palma, M.; Levin, J.; Lemaur, V.; Liscio, A.; Palermo, V.; Cornil, J.; Geerts, Y.; Lehmann, M.; Samori, P. *Adv. Mater.* **2006**, *18*, 3313.

(4) De Cupere, V.; Tant, J.; Viville, P.; Lazzaroni, R.; Osikowicz, W.; Salaneck, W. R.; Geerts, Y. H. *Langmuir* **2006**, *22*, 7798.

(5) Crispin, X.; Cornil, A.; Friedlein, R.; Okudaira, K. K.; Lemaur, V.; Crispin, A.; Kestemont, G.; Lehmann, M.; Fahlman, M.; Lazzaroni, R.; Geerts, Y.; Wendin, G.; Ueno, N.; Bredas, J. L.; Salaneck, W. R. *J. Am. Chem. Soc.* **2004**, *126*, 11889.

(6) Lemaur, V.; Da Silva Filho, D. A.; Coropceanu, V.; Lehmann, M.; Geerts, Y.; Piris, J.; Debije, M. G.; Van de Craats, A. M.; Senthilkumar, K.; Siebbeles, L. D. A.; Warman, J. M.; Bredas, J. L.; Cornil, J. *J. Am. Chem. Soc.* **2004**, *126*, 3271.

(7) Wu, J. S.; Pisula, W.; Mullen, K. *Chem. Rev.* **2007**, *107*, 718.

(8) Jackel, F.; Watson, M. D.; Mullen, K.; Rabe, J. P. *Phys. Rev. B* **2006**, *73*, 045423.

(9) Simpson, C. D.; Wu, J. S.; Watson, M. D.; Mullen, K. *J. Mater. Chem.* **2004**, *14*, 494.

(10) Kastler, M.; Pisula, W.; Laquai, F.; Kumar, A.; Davies, R. J.; Baluschev, S.; Garcia-Gutierrez, M. C.; Wasserfallen, D.; Butt, H. J.; Riekel, C.; Wegner, G.; Mullen, K. *Adv. Mater.* **2006**, *18*, 2255.

(11) Kastler, M.; Pisula, W.; Wasserfallen, D.; Pakula, T.; Mullen, K. *J. Am. Chem. Soc.* **2005**, *127*, 4286.

(12) Smolenyak, P. E.; Peterson, R. A.; Dunphy, D. R.; Mendes, S.; Nebesny, K. W.; O'Brien, D. F.; Saavedra, S. S.; Armstrong, R. N. *J. Porphyrins Phthalocyanines* **1999**, *3*, 620.

(13) Smolenyak, P.; Peterson, R.; Nebesny, K.; Torker, M.; O'Brien, D. F.; Armstrong, N. R. *J. Am. Chem. Soc.* **1999**, *121*, 8628.

(14) Smolenyak, P. E.; Osburn, E. J.; Chen, S. Y.; Chau, L. K.; OBrien, D. F.; Armstrong, N. R. *Langmuir* **1997**, *13*, 6568.

(15) Donley, C. L.; Xia, W.; Minch, B. A.; Zangmeister, R. A. P.; Drager, A. S.; Nebesny, K.; O'Brien, D. F.; Armstrong, N. R. *Langmuir* **2003**, *19*, 6512.

(16) Drager, A. S.; Zangmeister, R. A. P.; Armstrong, N. R.; O'Brien, D. F. *J. Am. Chem. Soc.* **2001**, *123*, 3595.

(17) Schouten, P. G.; Warman, J. M.; Dehaas, M. P.; Vannostrum, C. F.; Gelinck, G. H.; Nolte, R. J. M.; Copyn, M. J.; Zwikker, J. W.; Engel, M. K.; Hanack, M.; Chang, Y. H.; Ford, W. T. *J. Am. Chem. Soc.* **1994**, *116*, 6880.

(18) van de Craats, A. M.; Warman, J. M.; Fechtenkotter, A.; Brand, J. D.; Harbison, M. A.; Mullen, K. *Adv. Mater.* **1999**, *11*, 1469.

(19) van de Craats, A. M.; Stutzmann, N.; Bunk, O.; Nielsen, M. M.; Watson, M.; Mullen, K.; Chanzy, H. D.; Sirringhaus, H.; Friend, R. H. *Adv. Mater.* **2003**, *15*, 495.

(20) Pisula, W.; Menon, A.; Stepputat, M.; Lieberwirth, I.; Kolb, U.; Tracz, A.; Sirringhaus, H.; Pakula, T.; Mullen, K. *Adv. Mater.* **2005**, *17*, 684.

(21) Piris, J.; Debije, M. G.; Stutzmann, N.; Laursen, B. W.; Pisula, W.; Watson, M. D.; Bjornholm, T.; Mullen, K.; Warman, J. M. *Adv. Funct. Mater.* **2004**, *14*, 1053.

(22) Bredas, J. L.; Calbert, J. P.; da Silva, D. A.; Cornil, J. *Proc. Natl. Acad. Sci. U.S.A.* **2002**, *99*, 5804.

(23) Gattinger, P.; Rengel, H.; Neher, D.; Gurka, M.; Buck, M.; van de Craats, A. M.; Warman, J. M. *J. Phys. Chem. B* **1999**, *103*, 3179.

(24) Flora, W. H.; Mendes, S. B.; Doherty, W. J.; Saavedra, S. S.; Armstrong, N. R. *Langmuir* **2005**, *21*, 360.

(25) Zangmeister, R. A. P.; Smolenyak, P. E.; Drager, A. S.; O'Brien, D. F.; Armstrong, N. R. *Langmuir* **2001**, *17*, 7071.

(26) Sauer, T.; Arndt, T.; Batchelder, D. N.; Kalachev, A. A.; Wegner, G. *Thin Solid Films* **1990**, *187*, 357.

(27) Debe, M. K. *Appl. Surf. Sci.* **1982**, *14*, 1.

(28) Debe, M. K. *J. Appl. Phys.* **1984**, *55*, 3354.

(29) Allara, D. L.; Nuzzo, R. G. *Langmuir* **1985**, *1*, 52.

(30) Xia, W.; Minch, B. A.; Carducci, M. D.; Armstrong, N. R. *Langmuir* **2004**, *20*, 7998.

(31) Yang, X.; Nitzsche, S. A.; Hsu, S. L.; Collard, D.; Thakur, R.; Lillya, C. P.; Stidham, H. D. *Macromolecules* **1989**, *22*, 2611.

(32) Drager, A. S.; O'Brien, D. F. *J. Org. Chem.* **2000**, *65*, 2257.